

# Calcium alginate/activated carbon/humic acid tri-system porous fibers for removing tetracycline from aqueous solution

Qinye Sun<sup>&, 1</sup>, Heng Zheng<sup>&, 1</sup>, Yanhui Li<sup>1, 2, \*</sup>, Meixiu Li<sup>1</sup>, Qiuju Du<sup>1</sup>, Cuiping Wang<sup>1</sup>, Kunyan Sui<sup>1</sup>, Hongliang Li<sup>1</sup>, Yanzhi Xia<sup>1</sup>

<sup>1</sup>Qingdao University, State Key Laboratory of Bio-fibers and Eco-textiles, College of Mechanical and Electrical Engineering, Qingdao 266071, China

<sup>2</sup>Qingdao University, College of Mechanical and Electrical Engineering, 308 Ningxia Road, Qingdao 266071, China

<sup>&</sup>Qinye Sun and Heng Zheng contributed equally to this work

<sup>\*</sup>Corresponding author: e-mail: liyanhui537@163.com,

In this study, activated carbon and humic acid powder were fixed by the cross-linking reaction of sodium alginate. Calcium alginate/activated carbon/humic acid (CAH) tri-system porous fibers were prepared by the wet spinning method and freeze-dried for the removal of tetracycline in aqueous solution. Subsequently, the morphology and structure of CAH fibers were measured by scanning electron microscopy (SEM) and the Brunauer-Emmett-Teller (BET) method. The effect of pH, contact time, temperature and other factors on adsorption behavior were analyzed. The Langmuir and Freundlich isotherm models were used to fit tetracycline adsorption equilibrium data. The dynamics data were evaluated by the pseudo-second-order model, the pseudo-second-order model and the intraparticle diffusion model. Thermodynamic study confirmed that the adsorption of tetracycline on CAH fibers was a spontaneous process.

**Keywords:** Sodium alginate; Humic acid; Activated carbon; Adsorption; Tetracycline.

## INTRODUCTION

Antibiotics are not only commonly used in the treatment and prevention of human diseases<sup>1</sup>, but also widely used in animal husbandry and aquaculture to promote livestock growth<sup>2, 3</sup>.

The safety and efficacy of tetracycline (TC) makes it one of the most widely used antibiotics in the world. However, tetracycline is poorly absorbed from the gastrointestinal tract of animals<sup>4</sup>, with up to 50–80% excreted in animal feces. As a result, significant amounts of tetracycline enter the ecosystem, leading ultimately to the emergence of resistance genes<sup>5–7</sup>. The presence of tetracycline in the water environment can affect the activity and composition of microorganism communities and change their ecological structure<sup>8</sup>. Experimental results indicate that allergic reactions in some susceptible individuals are caused by antibiotic residues in food, and overuse of antibiotics can lead to super infection and drug resistance<sup>9</sup>. Therefore, it is a matter of urgency that efficient and clean methods are used to reduce and control environmental pollution caused by tetracycline.

Photocatalytic degradation<sup>10</sup>, ozonation<sup>11</sup> and adsorption are important methods for tetracycline removal. Among these methods, adsorption is particularly promising due to its low cost, non-toxicity and relative ease of use. Recent research shows that an adsorbent made by fixing copper ions with sodium alginate has high removal efficiency for tetracycline<sup>12</sup>, but the introduction of metal ions in the preparation process causes pollution to the environment. Experimental results show that activated carbon and graphene oxide have an adsorption effect on tetracycline<sup>13, 14</sup>, however the powder form is difficult to separate from the water solution, which means, once again, that its use causes environmental pollution. To overcome this problem, porous fibers are prepared by encapsulating activated carbon and humic acid powder with sodium alginate.

Activated carbon (AC), a form of graphite microcrystalline amorphous carbon with high degree of microporosity and huge specific surface area, is one of the most widely used materials for adsorbing dyes and pharmaceuticals<sup>15–17</sup>. Adding a large quantity of AC to the fibers can improve their adsorption capacity to TC, but when the quantity of AC is too large, it is difficult to continue to improve the adsorption capacity of the fibers. At this point, if a small amount of humic acid (HA) is added, the adsorption capacity of the fibers can be improved. HA is a type of complex natural macromolecular organic polymers that exist widely in nature<sup>18</sup>, formed by a series of processes such as microbial decomposition and the transformation of animal and plant remains<sup>19, 20</sup>. HA contains a plurality of functional groups, which allows for considerable complexation and ion exchange capacity<sup>21</sup>. However, its low dispersibility in aqueous solution limits its practical applications in environmental protection.

Sodium alginate (SA) is a kind of natural polysaccharide polymers<sup>22, 23</sup>. Through the exchange of divalent cations and sodium ions, a gel with three-dimensional network structure can be obtained, which can successfully encapsulate AC and HA powders, and facilitate the recovery of materials to improve the efficiency of adsorbents<sup>24</sup>. Experiments have shown that a large number of hydroxyl groups and carboxyl groups make the adsorption of dyes and other contaminants including methylene blue and metal ions possible<sup>25–27</sup>.

In this paper, aerogel adsorbent of calcium alginate/activated carbon/humic acid (CAH) porous fibers were prepared by wet spinning and vacuum freeze-drying methods<sup>28</sup>. The chemical structure and surface morphology of the fibers were characterized by scanning electron microscopy (SEM) and the Brunauer-Emmett-Teller (BET) method. The adsorption properties of the fibers for tetracycline removal were investigated by varying the temperature, amount of adsorbent, reaction time and the initial pH of the solution.

## MATERIALS AND METHODS

### Materials and Chemicals

TC (analytical reagent) was produced by Wuhan Lana White Pharmaceutical Factory and stored at 273 K. HA (No. 53680) was purchased from Tianjin Guangfu Fine Chemical Research Institute. Powdered AC was purchased from Hairuicheng Co., Ltd., Qingdao, China. Sodium alginate was obtained from Shanghai Aibi Chemical Reagent Co. All solutions were prepared with deionized water.

### Preparation of CAH fibers

The HA powder and sodium alginate powder were mixed in beaker so that the HA could be distributed more evenly in the sodium alginate fluid matrix. After adding deionized water to the beaker and stirring with the magnetic stirring device for 5 hours, activated carbon was added to the beaker and stirred for another 12 hours to obtain the black fluid mixture. The wet-spinning technique method is as follows: as soon as the mixture was injected into calcium chloride solution, ion exchange occurred rapidly between calcium ions and sodium alginate to form CAH fibers. The fibers were fully molded by leaving them to stand for 5 hours, followed by rinsing repeatedly with deionized water. After freezing the obtained fibers, the samples were obtained by freeze-drying. In order to determine the best proportion of SA, AC and HA, two experiments were conducted. SA/AC fibers were prepared with different mass ratios, and the optimum proportion of activated carbon was determined from the experiment. Subsequently, HA with different mass ratios was added to obtain the final ratio of SA, AC and HA.

### Characterization

The surface morphologies of CAH fibers were characterized by a high resolution scanning electron microscope (Quanta250 FEG, FEI, America). The BET equation (ASAP2460, micromeritics, Shanghai, China) was used to measure the specific surface area of CAH fibers by  $N_2$  adsorption isotherm.

### Adsorption studies

All experiments were carried out in a Vapour-bathing Constant Temperature Vibrator (SHZ-82A) with a rotational speed of 150 rpm. TC stock solution with a concentration of 1000 mg/L was stored at a temperature below 283 K. During the experiment, different concentrations of diluents were obtained by diluting the TC stock solution. Add 10 mg CAH fibers to 20 ml TC solution at different temperatures. After adsorption and equilibrium, CAH fibers were separated from TC solution. The equilibrium concentration of TC was measured by an ultraviolet-visible spectrophotometer. (TU-1810, Beijing Purkinje General Instrument Co., Ltd., Beijing) at wavelength of 360 nm.

The effects of TC concentration and ambient temperature on adsorption were simultaneously investigated. The initial concentration of TC solution ranged from 50 mg/L to 170 mg/L, with a total of 7 groups at temperatures of 303 K, 313 K and 323 K, respectively. In order to investigate the effect of initial pH on adsorption, the

initial pH value of TC solution (90 mg/L) was set from 2.3 to 7. Adsorbents with different doses (5–35 mg) were added to the TC solution (110 mg/L) to determine the effect of the amount of adsorbent on adsorption. The effect of contact time on TC adsorption was investigated by adding 300 mL TC solution (90 mg/L) to the beaker and the quantity of adsorbent was 150 mg. The residual TC concentration was determined by taking out the supernatant at a specific time interval. The adsorption capacity  $q_e$  (mg/g) and  $q_t$  (mg/g) were calculated based on the following equations:

$$q_e = \left( \frac{c_0 - c_e}{W} \right) \times V \quad (1)$$

$$q_t = \left( \frac{c_0 - c_t}{W} \right) \times V \quad (2)$$

Where  $c_0$  and  $c_e$  are the initial and equilibrium concentrations (mg/L) of TC solution, respectively;  $c_t$  is the residual concentration of TC at time  $t$ ;  $W$  is the mass of adsorbent (g) used in the corresponding adsorption experiments, and  $V$  is the volume of the solutions (L).

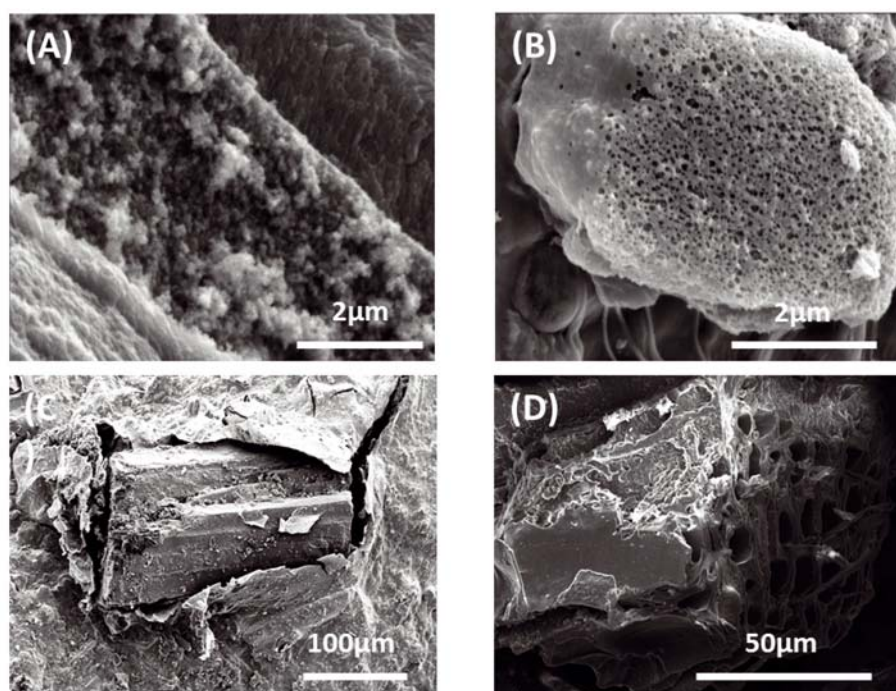
In order to obtain the optimal ratio of sodium alginate, activated carbon and humic acid, two groups of adsorption tests were conducted using 50 mg/L TC solution. In the first set of experiments: porous fibers with a mass ratio of SA to AC of 1:1–1:5 were prepared, and the best ratio was deemed to be 1:5 following the adsorption experiments. It was noteworthy that when the mass ratio of SA to AC is greater than 1:5, SA cannot completely encapsulate the activated carbon, and the formability of the fiber deteriorates. In the second set of experiments: preparation of SA, AC and HA mass ratio of 1:5:1 to 1:5:5 porous fibers led to an optimal ratio of 1:5:1. Then, the humic acid ratio was lowered to prepare fibers with a mass ratio of 1:5:0.5 and 1:5:0.25 for SA:AC:HA. The adsorption results showed that the optimal ratio of the three materials was 1:5:0.5.

## RESULTS AND DISCUSSION

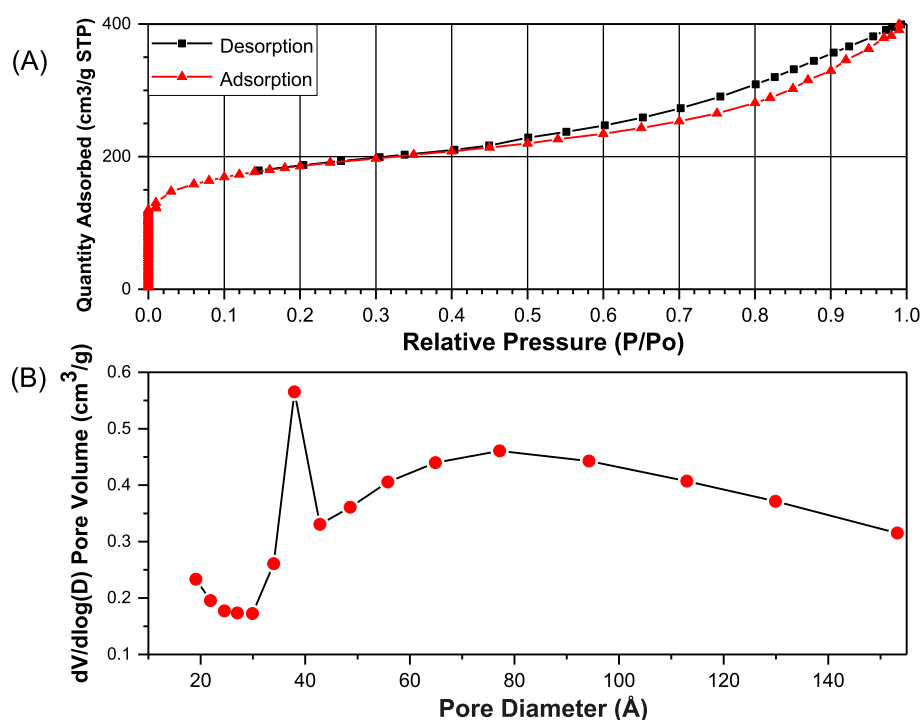
### Characterization of the prepared adsorbents

Figure 1 shows that the entire surface of CAH fibers is wrinkled, whilst the humic acid particles are dotted. The activated carbon particles are embedded on the fiber surface, piercing through several through-holes with large cross section. In particular, there are a number of porous hillocks distributed on the surface of CAH fibers. The surface of the hillocks is evenly distributed with the micropores. When the diameters between two adjacent holes become larger, the two holes combine and form a larger hole, which increases the surface area of the fiber.

The properties of adsorbents are closely correlated with pore volume and surface area. The  $N_2$  adsorption was performed on a CAH sample to evaluate its permanent porosity. Figure 2 A shows the adsorption hysteresis ring. It can be seen that CAH fibers have reversible type IV isotherm, which is one of the main characteristics of mesoporous materials<sup>29</sup>. The surface area of CAH fibers is 622 m<sup>2</sup>/g, as calculated by the brunauer-emmett-teller (BET) model. Figure 2 B shows the pore size distribu-



**Figure 1.** (A) Surface morphology of CAH fibers under SEM images, (B) Porous hillocks structure on CAH fibers, (C) Mosaic of activated carbon particles on CAH fibers, (D) Through-holes structure of activated carbon particles



**Figure 2.** (A) Isotherm Linear Plot, (B) BJH Desorption  $dV/d\log(D)$  Pore Volume

tion of CAH fibers. Most holes are mesopores, making up a proportion of 93.6%, whereas the proportions of micropores and macropores are 3.9% and 2.5%, respectively. CAH fibers are mainly distributed with narrow mesoporous pores, generally smaller than 10 nm in size, and the peak center of the pore size is mainly 3.79 and 7.71 nm. The addition of activated carbon can increase the surface area of CAH fibers. However, when the mass ratio of sodium alginate to activated carbon exceeds 1:5, the formability of the fiber deteriorates.

#### Effects of AC/HA dose and pH value on adsorption

Figure 3 A shows that activated carbon plays a major role in the adsorption of tetracycline by CAH fibers,

while a small amount of humic acid can greatly improve the adsorption effect of the adsorbent. Figure 3 B shows that when the proportion of humic acid exceeds 0.5, the adsorption efficiency decreases. This may be attributed to an excessive HA content bringing about a decrease in the amount of AC in fibers of the same weight. On the other hand, when the proportion is less than 0.5, the amount of humic acid is too small to play such a role.

Humic acid has strong complexation with tetracycline and shows pH dependence<sup>30</sup>, so the adsorption efficiency of CAH fibers on tetracycline is affected by pH, as shown in the Figure 4 A. There are ionizable groups including  $-\text{COOH}$ ,  $-\text{OH}$  and  $-\text{NH}_2$ <sup>31</sup> in TC molecule,

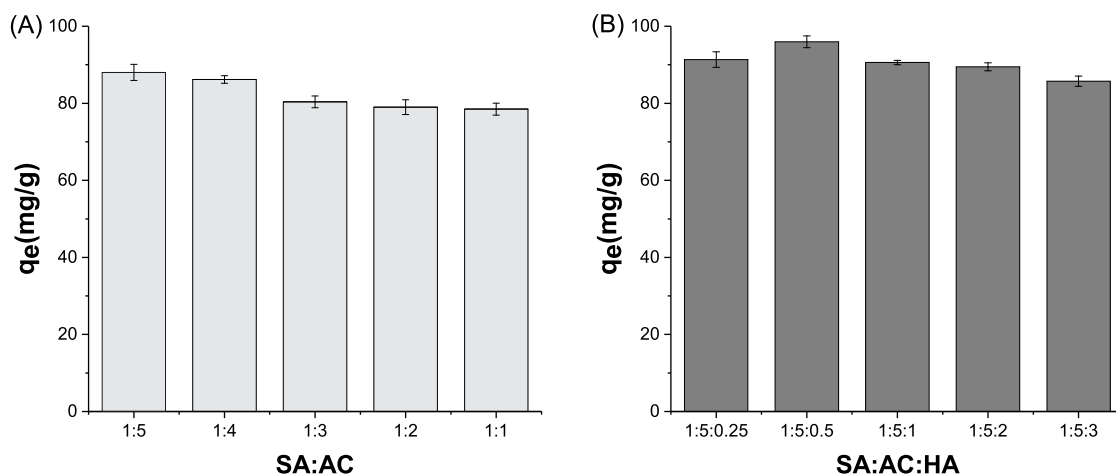


**Figure 3.** Effect of AC/HA dose on adsorption capacity of CAH fibers: (A) different mass ratios of AC, (B) different mass ratios of HA

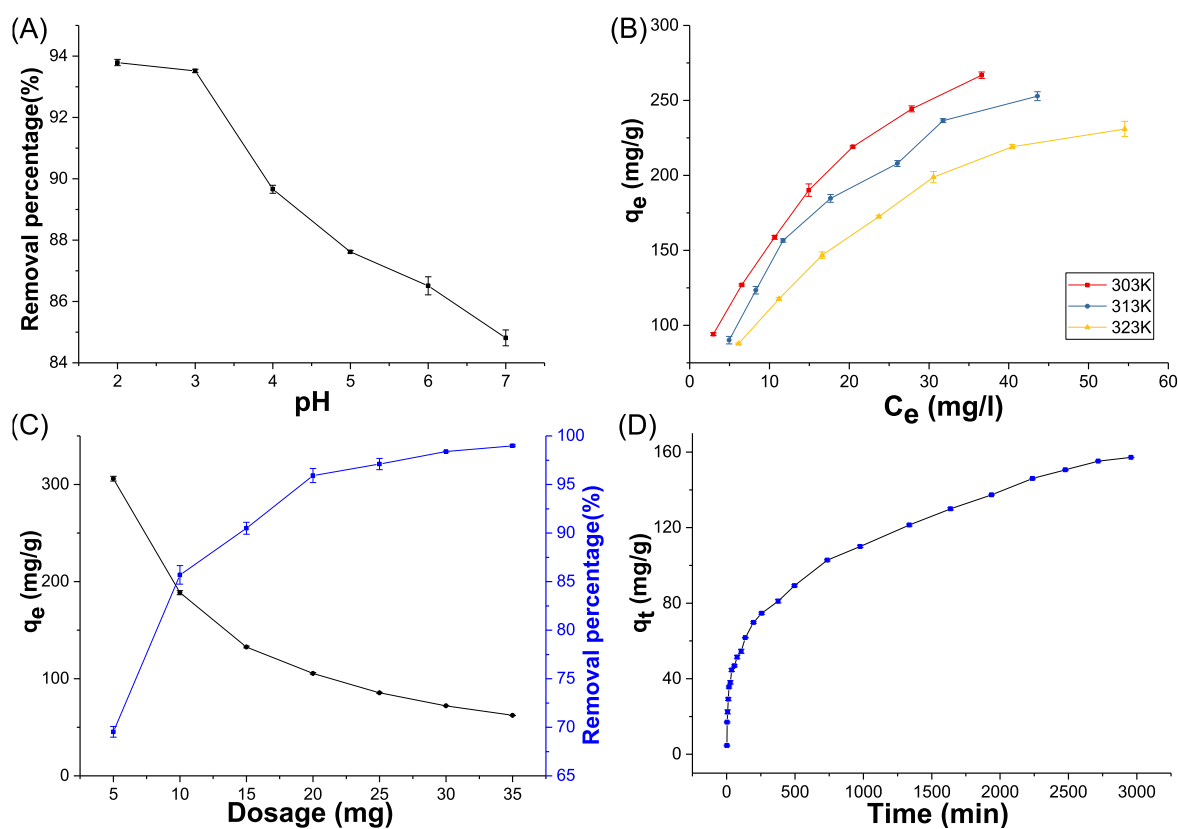


**Figure 4.** Effect of various experimental parameters on adsorption capacity of CAH fibers: (A) pH, (B) temperature, (C) dosage, (D) contact time

which are dissociated under different conditions, so that TC finally comes to form cations, zwitterions and anionic<sup>32,33</sup>. When the solution environment is acidic, the main forms of tetracycline are cations and zwitterions, which can interact with the humic acid in the fibers through hydrogen bond or electrostatic attraction<sup>34</sup>. The adsorption capacity increased as pH decreased. When  $\text{pH} \leq 3$ , the trend of increasing adsorption capacity slowed, due to the competition between  $\text{H}^+$  and tetracycline in the solution for the binding sites of humic acid. When pH ranged from 4.3 to 6.5, tetracycline still present in the form of zwitterion, but the adsorption efficiency decreased. As the carboxylic groups in humic acid became progressively deprotonated, there was decreased carboxylic acid hydrogen bonding, which led to a reduction in adsorption efficiency.

#### Effects of temperature

Temperature has a direct effect on the diffusion rate of tetracycline and adsorbent performance, so it is an important factor in the adsorption process. The influence of temperature and TC initial concentrations on the adsorption effect is shown in Figure 4 B, which was carried out at 303, 313 and 323 K, respectively. The results showed that when the temperature was increased from 303 K to 323 K, the adsorption capacity of the adsorbent decreased from 266.78 mg/g to 230.92 mg/g. This may be due to a reduction in the number of available binding sites of activated carbon and humic acid to tetracycline. Also, the adsorption capacity of CAH fibers to TC solution of the same concentration decreased, as temperature rose, indicating that the adsorption reaction is an exothermic process. For the initial concentration

of TC, as the concentration gradient increased, the adsorption capacity increased from 94.07 mg/g to 266.78 mg/g at 303 K.

### Effects of adsorbent dosage

The amount of adsorbent is an important parameter affecting adsorption efficiency. Figure 4 C shows the influence of different adsorbent dosages on the adsorption capacity and removal rate. It can be seen that as the amount of adsorbent increases, the adsorption capacity decreases rapidly, but the removal rate increases, reaching a maximum of 98.8%. This may be due to an increase in the number of sites capable of binding to TC. However, even when the number of available binding sites increases, a reduction in the utilization of binding sites would result in a decrease in adsorption capacity. Once the binding of the adsorption sites to TC reaches saturation, removal efficiency no longer increases<sup>34</sup>.

### Adsorption isotherm

Adsorption isotherm can be used to explain the essence of the adsorption behavior of CAH fibers towards tetracycline to better understand the relationship between the adsorption amount and the residual concentration. The most commonly used models for studying adsorption equilibrium are the Langmuir model and the Freundlich model. The Langmuir model assumes the adsorption process takes place on a uniform surface and a single layer.  $c_e$  (mg/L) represents the equilibrium concentration, that is, the concentration of the solution after adsorption equilibrium, and  $q_e$  (mg/g) is the equilibrium adsorption capacity, which reflects the change of solution concentrations caused by the adsorbent per unit mass. After fitting the models, the maximum adsorption  $q_{max}$  (mg/g) and Langmuir constant  $k_L$  (L/g) can be calculated. The Langmuir model equation is expressed as follows<sup>35</sup>:

$$\frac{c_e}{q_e} = \frac{c_e}{q_{max}} + \frac{1}{q_{max}k_L} \quad (3)$$

**Table 1.** Adsorption isotherm model parameters of CAH fibers adsorbed TC

TEMP(K)	Langmuir			Freundlich			
	$q_{max}$ (mg/g)	$k_L$ (L/mg)	$R^2$	$R_L$	$k_F$ (L/mg)	$1/n$	$R^2$
303	333.33	0.098	0.983	0.056–0.169	58.399	0.428	0.995
313	330.03	0.073	0.995	0.074–0.215	45.304	0.472	0.974
323	303.95	0.059	0.994	0.090–0.253	39.078	0.461	0.984

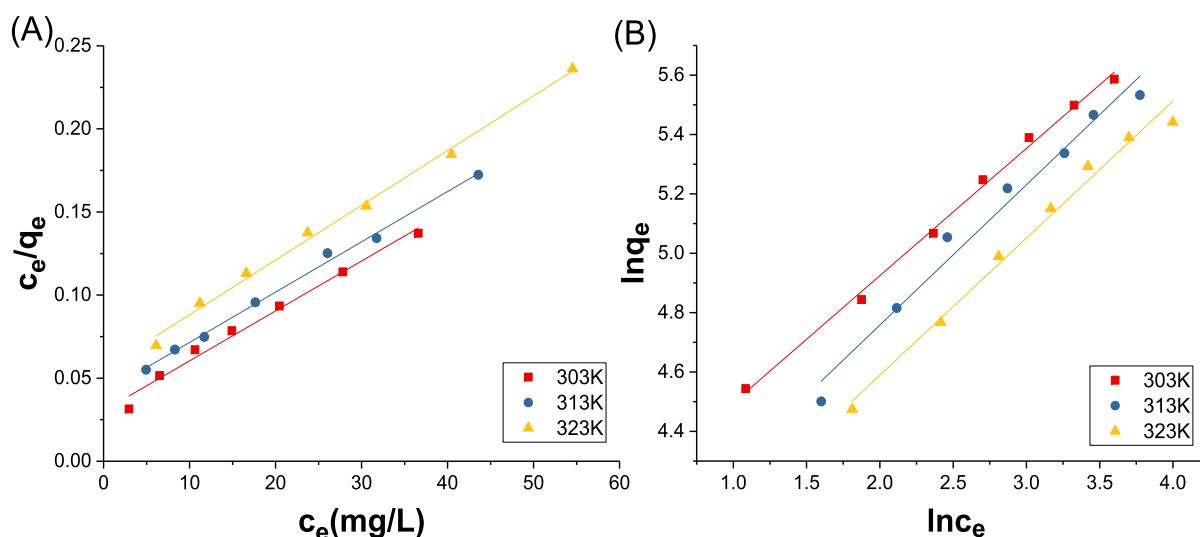


**Figure 5.** The equilibrium isotherms of TC on CAH fibers at 303, 313 and 323 K: (A) Isotherm obtained by the Langmuir model, (B) Isotherm obtained by the Freundlich model

At 303, 313 and 323 K, the maximum single-layer adsorption capacity is similar. The dimensionless constant  $R_L$  can be used to evaluate whether the adsorption process is favorable.  $C_0$  is the initial concentration of the solution, and the equation is as follows:

$$R_L = \frac{1}{1 + c_0 k_L} \quad (4)$$

As listed in Table 1, the  $R_L$  values are all between 0 and 1, indicating that the adsorption process is favorable, with CAH fibers having a good adsorption ability towards TC<sup>36</sup>. The Freundlich model can be applied to describe both single layer adsorption and heterogeneous surface adsorption.  $k_F$  and  $n$  are Freundlich constants, where  $k_F$  is related to the adsorption affinity of the adsorbent, and  $n$  indicates the supporting force of the adsorption process, respectively. The Freundlich isothermal model is shown in the equation below (9)<sup>37</sup>:

$$\ln q_e = \ln k_F + \frac{1}{n} \ln c_e \quad (5)$$

As shown in Figure 5, the  $R^2$  values obtained by fitting the adsorption isotherm with the two models are quite high, indicating that both models could fit the adsorption process well. The  $1/n$  value calculated by the Freundlich model equation is less than 1, indicating that the adsorption process was effective.

### Adsorption kinetic study

The study of adsorption kinetics is important for describing the adsorption rate and the control mechanism of adsorption. 150 mg CAH fibers were added to 300 mL TC solution with an initial concentration of 90 mg/L at 303 K. As shown in Figure 4 D, the adsorption rate is very fast in the first 8 minutes, which could be explained by the large number of adsorption sites on CAH fibers in the initial stage. As time goes on, however, the adsorption rate gradually slows until equilibrium is

reached, because the number of adsorption sites and the amount of TC in the solution are both dropping, and the remaining TC needs to spend more time finding binding sites that can form hydrogen bonds.

In this paper, the pseudo-first-order model, the pseudo-second-order model and the intra-particle diffusion model are used to analyze and fit the experimental data, respectively. The mathematical expression of the pseudo-first-order model and pseudo-second-order model is as follows<sup>38,39</sup>:

$$\log(q_e - q_t) = \log q_e - \frac{k_1}{2.303} t \quad (6)$$

$$\frac{t}{q_t} = \frac{1}{k_2 q_e^2} + \frac{t}{q_e} \quad (7)$$

Where  $k_1$  (1/min) is the adsorption rate constant for the pseudo-first-order adsorption process,  $k_2$  (g/mg·min) is the corresponding kinetic constant,  $q_e$  and  $q_t$  are the adsorption amount of TC (mg/g) under equilibrium conditions and the adsorption amount of TC (mg/g) at a specific time  $t$  (min), respectively. The values of  $k_1$ ,  $k_2$ ,  $q_e$  are determined by fitting the slope and intercept of the line. All the above data are listed in Table 2, and the results showed that the quasi-second order model describes the experimental data well<sup>40</sup>. The correlation coefficient of the pseudo-second order model is 0.98, which is much higher than that of the pseudo-first-order model. Compared with the equilibrium adsorption calculated by the pseudo-first-order model (135.80 mg/g), the equilibrium adsorption calculated by the pseudo-second-order model (156.98 mg/g) was closer to the experimental adsorption (157.19 mg/g). It can be seen from Figure 6 that the pseudo-second-order model can better fit the data.

**Table 2.** The kinetic constants of adsorption of TC on CAH fibers

Kinetic model	Parameters	Values
Pseudo-first-order model	$k_1$ (min <sup>-1</sup> )	$1.316 \times 10^{-3}$
	$q_e$ (mg/g)	135.806
	$R^2$	0.9136
Pseudo-second-order model	$k_2$ (g/mg·min)	$3.391 \times 10^{-5}$
	$q_e$ (mg/g)	156.985
	$R^2$	0.9806
Intraparticle diffusion model	$k_{1d}$	10.6713
	$C_1$	-7.3975
	$R_1^2$	0.9469
	$k_{2d}$	2.3977
	$C_2$	32.244
	$R_2^2$	0.9933

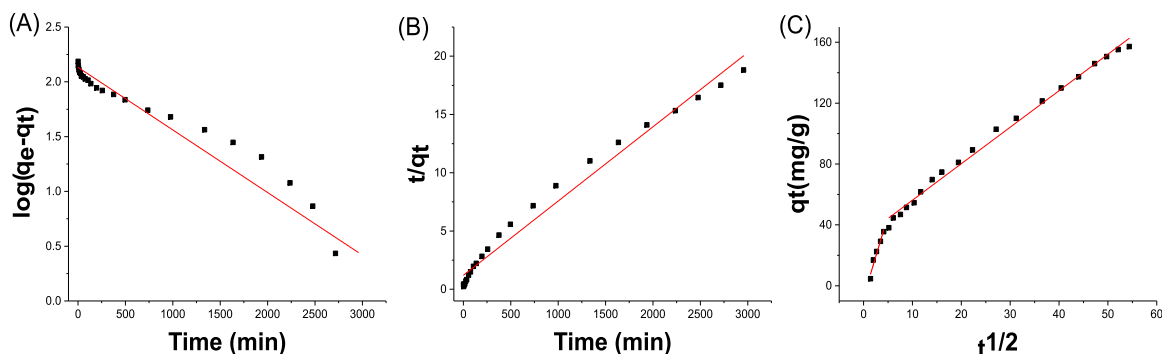


**Figure 6.** Adsorption kinetics of TC adsorbed by CAH fibers: (A) pseudo-first-order model, (B) pseudo-second-order model, (C) intra-particle diffusion model

In order to further study the adsorption process of TC on CAH fibers, the diffusion mechanism is analyzed by the intra-particle diffusion model. Generally, the fitting line does not pass through the origin, and the adsorption process is controlled by multiple stages, generally divided into three stages: (1) external particle diffusion stage; (2) pore diffusion stage; (3) adsorption reaction stage. The intra-particle diffusion model is used to describe the rate control step of the whole process, and the formula is<sup>41</sup>:

$$q_t = k_{id} t^{1/2} + C_i \quad (8)$$

Where,  $k_{id}$  is the particle internal diffusion constant (mg/g min<sup>1/2</sup>),  $q_t$  is the adsorption capacity at time  $t$  (min), and  $C_i$  is a parameter related to boundary layer and thickness. Figure 6 C shows that the adsorption process is divided into two stages. In the first stage, the fitting line is steep and there are a large number of adsorption sites on the surface of CAH fiber with a high adsorption rate, which is mainly attributable to macroporous diffusion. The second stage is the gradual adsorption stage with a small slope. Intra-particle diffusion is a step that controls the adsorption rate, which is mainly attributable to microporous diffusion<sup>42,43</sup>. And  $k_{1d}$  (10.6713 mg/g min<sup>1/2</sup>) is significantly higher than  $k_{2d}$  (2.3977 mg/g min<sup>1/2</sup>), indicating that external diffusion plays a more important role in adsorption kinetics.

#### Adsorption thermodynamic study

In order to study the energy change of CAH fibers on TC adsorption, the thermodynamic data of the adsorption process are calculated at different temperatures. Enthalpy ( $\Delta H$ ) and entropy ( $\Delta S$ ) are obtained using the following equations<sup>44</sup>:

$$\Delta G = \Delta H - T\Delta S \quad (9)$$

$$\ln\left(\frac{q_e}{C_e}\right) = -\frac{\Delta H}{RT} + \frac{\Delta S}{R} \quad (10)$$

Where  $R$  is the universal gas constant (8.314 J/K) and  $T$  represents the absolute temperature in Kelvin (K). A straight line can be obtained by plotting  $1/T$  and  $\ln(q_e/C_e)$ ,  $\Delta H$  and  $\Delta S$  can be calculated according to the linear slope and intercept, respectively. The specific thermodynamic parameters are listed in Table 3. The value of  $\Delta H$  is -29.32 kJ/mol which means that exothermic reactions take place between the adsorbent and TC, with low temperatures more favorable for adsorption.

**Table 3.** Thermodynamic parameters at different temperatures

TEMP(K)	$\Delta G$ (kJ/mol)	$\Delta H$ (kJ/mol)	$\Delta S$ (J/mol K)
303	-7.74	-29.32	-71.237
313	-7.02		
323	-6.31		

$\Delta G$  less than zero indicates that the adsorption process is spontaneous.

## CONCLUSIONS

The experimental results in this paper showed that CAH fibers can effectively remove TC from aqueous solution. The optimal ratio of SA, AC and HA was 1:5:0.5, and the maximum adsorption capacity of the porous fibers was up to 95.948 mg/g after adsorption of the TC solution with a concentration of 50 mg/L. Adsorption was more favorable at a lower temperature (303 K) and in an acidic solution environment. At 303 K, the maximum adsorption capacity of CAH fibers for TC was 333.33 mg/g. Thermodynamic parameters showed that the adsorption process of TC on CAH fibers was spontaneous and exothermic. The isothermal parameters and kinetics were well described by the Langmuir isotherm model and the pseudo-second-order model, respectively. Based on these analyses, CAH fiber is an environmentally friendly material that can effectively remove TC from aqueous solution and is easily separated from the water environment, which has broad application prospects.

## ACKNOWLEDGMENTS

This work was supported by the National Natural Science Foundation of China (51672140), Natural Science Foundation of Shandong Province (ZR2015EM038), Taishan Scholar Program of Shandong Province (201511029).

## LITERATURE CITED

- Ahmed, M.B., Zhou, J.L., Ngo, H.H. & Guo, W. (2015). Adsorptive removal of antibiotics from water and wastewater: Progress and challenges. *Sci. Total Environ.* 532, 112–126. DOI: 10.1016/j.scitotenv.2015.05.130.
- Gao, Y., Li, Y., Zhang, L., Huang, H., Hu, J., Shah, S.M. & Su X. (2012). Adsorption and removal of tetracycline antibiotics from aqueous solution by graphene oxide. *J. Colloid & Interf. Sci.* 368, 540–546. DOI: 10.1016/j.jcis.2011.11.015.
- Tayeri, V., Seidavi, A., Asadpour, L. & Phillips, C.J.C. (2018). A comparison of the effects of antibiotics, probiotics, synbiotics and prebiotics on the performance and carcass characteristics of broilers. *Veter. Res. Commun.* 42, 1–13.
- Wang, Q., Li, X., Yang, Q., Chen, Y. & Du, B. (2019). Evolution of microbial community and drug resistance during enrichment of tetracycline-degrading bacteria. DOI: 10.1016/j.ecoenv.2019.01.047. DOI: 10.1016/j.ecoenv.2019.01.047.
- Homem, V. & Santos, L. (2011). Degradation and removal methods of antibiotics from aqueous matrices – a review. *J. Environ. Manag.* 92, 2304–2347. DOI: 10.1016/j.jenvman.2011.05.023.
- Yang, Y., Liu, W., Xu, C., Wei, B. & Wang, J. (2017). Antibiotic resistance genes in lakes from middle and lower reaches of the Yangtze River, China: Effect of land use and sediment characteristics. *Chemosphere* 178, 19–25. DOI: 10.1016/j.chemosphere.2017.03.041.
- Le, X.T., Munekage, Y. & Kato, S. (2005). Antibiotic resistance in bacteria from shrimp farming in mangrove areas. *Sci. The Total Environ.* 349, 95–105. DOI: 10.1016/j.scitotenv.2005.01.006.

- Qiu, W., Sun, J., Fang, M., Luo, S., Tian, Y., Dong, P., Xu, B. & Zheng, C. Occurrence of antibiotics in the main rivers of Shenzhen, China: Association with antibiotic resistance genes and microbial community. *Sci. The Total Environ.* DOI: 10.1016/j.scitotenv.2018.10.398.
- Jin, H., Kumar, A.P., Paik, D.-H., Ha, K.-Ch., Yoo, Y.-J. & Lee Y.-Ill. (2010). Trace analysis of tetracycline antibiotics in human urine using UPLC-QToF mass spectrometry. *Microchem. J.* 94, 139–147. DOI: 10.1016/j.microc.2009.10.010.
- Rong, H., Xin, X., Zuo, X., Nan, J. & Zhang, W. (2012). Efficient adsorption and visible-light photocatalytic degradation of tetracycline hydrochloride using mesoporous BiOI microspheres. *J. Hazard. Mater.* 209–210, 137–145. DOI: 10.1016/j.jhazmat.2012.01.006.
- Wang, L., Ben, W., Li, Y., Liu, C. & Qiang, Z. (2018). Behavior of tetracycline and macrolide antibiotics in activated sludge process and their subsequent removal during sludge reduction by ozone. *Chemosphere* 206, 184–191. DOI: 10.1016/j.chemosphere.2018.04.180.
- Zhang, X., Lin, X., He, Y., Chen, Y., Luo, X. & Shang, R. (2019). Study on adsorption of tetracycline by Cu-immobilized alginate adsorbent from water environment. *Int. J. Biol. Macromol.* 124, 418–428. DOI: 10.1016/j.ijbiomac.2018.11.218.
- Zhang, D., Yin, J., Zhao, H., Zhu, J. & Wang, C. (2015). Adsorption and removal of tetracycline from water by petroleum coke-derived highly porous activated carbon. *J. Environ. Chem. Engin.* 3, 1504–1512. DOI: 10.1016/j.jece.2015.05.014.
- Liu, P., Liu, W.J., Jiang, H., Chen, J.J., Li, W.W. & Yu, H.Q. (2012). Modification of bio-char derived from fast pyrolysis of biomass and its application in removal of tetracycline from aqueous solution. *Biores. Technol.* 121, 235–240. DOI: 10.1016/j.biortech.2012.06.085.
- Farooq, M., Bell, A.H., Almustapha, M.N. & Andresen, J.M. (2017). Bio-methane from an-aerobic digestion using activated carbon adsorption. *Anaerobe* 46, 33–40. DOI: 10.1016/j.anaerobe.2017.05.003.
- Yuan, G., Yue, Q., Gao, B., Sun, Y., Wang, W., Qian, L. & Yan, W. (2013). Preparation of high surface area-activated carbon from lignin of papermaking black liquor by KOH activation for Ni(II) adsorption. *Chem. Engin. J.* 217, 345–353. DOI: 10.1016/j.cej.2012.09.038.
- Mahdavi, M., Ebrahimi, A., Mahvi, A.H., Fatehizadeh, A. & Azarpira, H. (2018). Experimental data for aluminum removal from aqueous solution by raw and iron-modified granular activated carbon. *Data in Brief.* 17, 731–738. DOI: 10.1016/j.dib.2018.01.063.
- Hao, B.P. & Zheng, P.S. (2010). Suggestion on Utilization and Development of Humic Acid in Ecological Agriculture Construction. *J. Shanxi Agric. Sci.* DOI: 10.1080/00949651003724790. DOI: 10.1080/00949651003724790.
- Kloster, N. & Avena, M. (2015). Interaction of humic acids with soil minerals: adsorption and surface aggregation induced by Ca<sup>2+</sup>. *Environ. Chem.* 12, 37–39. DOI: 10.1071/EN14157.
- Pils, J.R. & Laird, D.A. (2007). Sorption of tetracycline and chlortetracycline on K- and Ca-saturated soil clays, humic substances, and clay-humic complexes. *Environ. Sci. & Technol.* 41, 1928.
- Tombácz, E., Dobos, Á., Szekeres, M., Narres, H.D., Klumpp, E. & Dékány, I. (2000). Effect of pH and ionic strength on the interaction of humic acid with aluminium oxide. *Colloid & Polym. Sci.* 278, 337–345. DOI: 10.1007/s003960050522.
- Zhang, H., Omer, A.M., Hu, Z., Ly, Y., Ji, C. & Ouyang, X.K. (2019). Fabrication of magnetic bentonite/carboxymethyl chitosan/sodium alginate hydrogel beads for Cu (II) adsorption. *Internat. J. Biolog. Macromol.* 135, 490.
- Dechojarassri, D., Omote, S., Nishida, K., Omura, T. & Tamura, H. (2018). Preparation of alginate fibers coagulated by calcium chloride or sulfuric acid: Application to the adsorption of Sr<sup>2+</sup>. *J. Hazard. Mater.* 355, 154–161.

24. Sarmiento, B., Martins, S., Ribeiro, A., Veiga, F., Neufeld, R. & Ferreira, D. (2006). Development and Comparison of Different Nanoparticulate Polyelectrolyte Complexes as Insulin Carriers. *Internat. J. Peptide Res. & Therap.* 12, 131–138. DOI: 10.1007/s10989-005-9010-3.
25. Jing, Y., Wang, J. & Jiang, Y. (2016). Removal of Uranium from Aqueous Solution by Alginate Beads. *Nuclear Engin. & Technol.* 49, S1738573316301826. DOI: 10.1016/j.net.2016.09.004.
26. Olad, A. & Azhar, F.F. (2014). A study on the adsorption of chromium (VI) from aqueous solutions on the alginate-montmorillonite/polyaniline nanocomposite. *Desal. & Water Treatm.* 52, 2548–2559. DOI: 10.1080/19443994.2013.794711.
27. Pawar, R.R., Lalmunsiama, Gupta, P., Sawant, S.Y., Shahmoradi, B. & Lee, S.M. (2018). Porous synthetic hectrite clay-alginate composite beads for effective adsorption of methylene blue dye from aqueous solution. *Internat. J. Biol. Macromol.* 114, 1315–1324. DOI: 10.1016/j.ijbiomac.2018.04.008.
28. Foroughi, J., Spinks, G.M., Wallace, G.G & Whitten, P.G. (2008). Production of polypyrrole fibres by wet spinning. *Synt. Metals.* 158, 104–107. DOI: 10.1016/j.synthmet.2007.12.008.
29. Jiaguo, Y.U., Wang, S., Low, J. & Xiao, W. (2013). Enhanced photocatalytic performance of direct Z-scheme g-C<sub>3</sub>N<sub>4</sub>-TiO<sub>2</sub> photocatalysts for the decomposition of formaldehyde in air. *Phys. Chem. Chem. Phys.* 15, 16883–16890.
30. Gu, C., Karthikeyan, K.G., Sibley, S.D. & Pedersen, J.A. (2007). Complexation of the antibiotic tetracycline with humic acid. *Chemosphere* 66, 1494–1501.
31. Chen, L.C., Lei, S., Wang, M.Z., Yang, J. & Ge, X.W. (2016). Fabrication of macroporous polystyrene/graphene oxide composite monolith and its adsorption property for tetracycline. *Chin. Chem. Letters.* 27, 511–517. DOI: 10.1016/j.ccl.2016.01.057.
32. Choi, K.J., Kim, S.G. & Kim, S.H. (2008). Removal of antibiotics by coagulation and granular activated carbon filtration. *J. Hazard. Mater.* 151, 38–43. DOI: 10.1016/j.jhazmat.2007.05.059.
33. Zhao, Y., Xueyuan, G.U., Gao, S., Geng, J. & Wang, X. (2012). Adsorption of tetracycline (TC) onto montmorillonite: Cations and humic acid effects. *Geoderma* 183–184, 12–18. DOI: 10.1016/j.geoderma.2012.03.004.
34. Dong, C., Zeng, Z., Zeng, Y., Fan, Z. & Wang, M. (2016). Removal of methylene blue and mechanism on magnetic  $\gamma$ -Fe<sub>2</sub>O<sub>3</sub>/SiO<sub>2</sub> nanocomposite from aqueous solution. *Water Res. & Ind.* 15, 1–13. DOI: 10.1016/j.wri.2016.05.003.
35. Langmuir, I. The constitution and fundamental properties of solids and liquids, DOI: 10.1016/s0016-0032(17)90938-x. DOI: 10.1016/s0016-0032(17)90938-x.
36. Kooh, M.R.R., Dahri, M.K., Lim, L.B. L., Lim, L.H. & Malik, O.A. (2016). Batch adsorption studies of the removal of methyl violet 2B by soya bean waste: isotherm, kinetics and artificial neural network modelling. *Environ. Earth Sci.* 75, 783. DOI: 10.1007/s12665-016-5582-9.
37. Gupta, V.K., Pathania, D., Sharma, S., Agarwal, S. & Singh, P. (2013). Remediation of noxious chromium (VI) utilizing acrylic acid grafted lignocellulosic adsorbent. *J. Molec. Liquids* 177, 343–352. DOI: 10.1016/j.molliq.2012.10.017.
38. Doğan, M., Alkan, M., Demirbaş, Ö., Özdemir, Y. & Özmetin, C. (2006). Adsorption kinetics of maxilon blue GRL onto sepiolite from aqueous solutions. *Chem. Engin. J.* 124, 89–101. DOI: 10.1016/j.cej.2006.08.016.
39. Ho, Y.S. & Chiang, C.C. (2001). Sorption Studies of Acid Dye by Mixed Sorbents. *Adsorp. J. The Internat. Ads. Soc.* 7, 139–147. DOI: 10.1023/A:1011652224816.
40. Jiang, L.H., Liu, Y.G., Zeng, G.M., Xiao, F.Y., Hu, X.J., Hu, X., Wang, H., Li, T.T., Zhou, L. & Tan, X.F. (2016). Removal of 17 $\beta$ -estradiol by few-layered graphene oxide nanosheets from aqueous solutions: External influence and adsorption mechanism. *Chem. Engin. J.* 284, 93–102. DOI: 10.1016/j.cej.2015.08.139.
41. Elmoubarki, R., Mahjoubi, F.Z., Tounsadi, H., Moustadraf, J., Abdennouri, M., Zouhri, A., Albani, A.E. & Barka, N. (2015). Adsorption of textile dyes on raw and decanted Moroccan clays: Kinetics, equilibrium and thermodynamics. *Water Res. & Ind.* 9, 16–29. DOI: 10.1016/j.wri.2014.11.001.
42. Wu, F.C., Tseng, R.L. & Juang, R.S. (2005). Comparisons of porous and adsorption properties of carbons activated by steam and KOH. *J. Colloid Interf. Sci.* 283, 49–56. DOI: 10.1016/j.jcis.2004.08.037.
43. Martins, A.C., Pezoti, O., Cazetta, A.L., Bedin, K.C., Yamazaki, D.A.S., Bandoch, G.F.G., Asefa, T., Visentainer, J.V. & Almeida, V.C. (2015). Removal of tetracycline by NaOH-activated carbon produced from macadamia nut shells: Kinetic and equilibrium studies. *Chem. Engin. J.* 260, 291–299. DOI: 10.1016/j.cej.2014.09.017.
44. Neghlani, P.K., Rafizadeh, M. & Taromi, F.A. (2011). Preparation of aminated-polyacrylonitrile nanofiber membranes for the adsorption of metal ions: Comparison with microfibers. *J. Hazard. Mater.* 186, 182–189.